Biophysical Journal
Article

Biophysical Society

Binding equations for the lipid composition dependence of peripheral membrane-binding proteins

Daniel Kerr,[1] Tiffany Suwatthee,[1] Sofiya Maltseva,[1] and Ka Yee C. Lee[1,2,*]
[1]Department of Chemistry, The University of Chicago, Chicago, Illinois and [2]James Franck Institute, The University of Chicago, Chicago, Illinois

ABSTRACT The specific recognition of peripheral membrane-binding proteins for their target membranes is mediated by a complex constellation of various lipid contacts. Despite the inherent complexities of the heterogeneous protein-membrane interface, the binding dependence of such proteins is, surprisingly, often reliably described by simple models such as the Langmuir Adsorption Isotherm or the Hill equation. However, these models were not developed to describe associations with two-dimensional, highly concentrated heterogeneous ligands such as lipid membranes. In particular, these models fail to capture the dependence on the lipid composition, a significant determinant of binding that distinguishes target from non-target membranes. In this work, we present a model that describes the dependence of peripheral proteins on lipid composition through an analytic expression for their association. The resulting membrane-binding equation retains the features of these simple models but completely describes the binding dependence on multiple relevant variables in addition to the lipid composition, such as protein and vesicle concentration. Implicit in this lipid composition dependence is a new form of membrane-based cooperativity that significantly differs from traditional solution-based cooperativity. We introduce the Membrane-Hill number as a measure of this cooperativity and describe its unique properties. We illustrate the utility and interpretational power of our model by analyzing previously published data on two peripheral proteins that associate with phosphatidylserine-containing membranes: The transmembrane immunoglobulin and mucin domain-containing protein 3 (TIM3) that employs calcium in its association, and milk fat globulin epidermal growth factor VIII (MFG-E8) which is completely insensitive to calcium. We also provide binding equations for systems that exhibit more complexity in their membrane-binding.

SIGNIFICANCE The association of peripheral membrane-binding proteins with their target membranes is important in multiple physiological processes. These associations can be highly sensitive to the lipid composition of the membrane, but quantitative characterization of this dependence has been difficult. We present a general model that quantitatively describes the lipid composition dependence of protein-membrane binding. This model gives rise to a new notion of cooperativity specific for protein-membrane binding. We introduce the Membrane-Hill number to quantify this cooperativity and discuss its implications for lipid composition dependence in a variety of systems.

INTRODUCTION

The binding of peripheral membrane-binding proteins with lipid membranes underlies multiple physiological processes from the clearance of apoptotic cell to the pruning of synapses (1–4). Many such proteins in this class recognize their target membranes through the composition, packing density, curvature, or other physicochemical properties. Complementarily, cells tune their composition and physical properties to effect these associations, as in, for example, the exposure of phosphatidylserine (PS) on the surface of apoptotic membranes to recruit phagocytes (1,2,5,6). As the characterization of the composition of cell membranes has steadily increased in precision and scope (5,7–11), the study of peripheral proteins has not kept pace with this growing complexity.

The lipid composition dependence of the binding of several peripheral proteins has long been established. For example, the C2-domain-containing proteins, such as

Submitted November 17, 2023, and accepted for publication February 29, 2024.

*Correspondence: kayeelee@uchicago.edu

Editor: Frederick A. Heberle.
https://doi.org/10.1016/j.bpj.2024.02.031

Box 1. Glossary of terms

CONCENTRATIONS

[L] – Concentration of all lipid species that are unassociated with membrane-bound protein

[P] – Concentration of free protein in solution

$[P]_{bound}$, [PB] – Concentration of membrane-bound protein/protein-bound lipid ensemble binding sites

$[P]_{bound,max}$, $[PB]_{max}$ – Concentration of membrane-bound protein/protein-bound lipid ensemble binding sites when the membrane is saturated

[B] – Concentration of unbound lipid ensemble binding sites

$[Ca^{2+}]$ – Concentration of free divalent cation in solution

{S} – Membrane mole fraction of the preferred lipid species *S*

{C} – Membrane mole fraction of unpreferred lipid species *C*

GENERAL BINDING PARAMETERS

$K_{D,L}$ – Dissociation constant of protein-membrane association with respect to [L]

$K_{D,P}$ – Dissociation constant of protein-membrane association with respect to [P]

$K_{D,B}$ – Dissociation constant of protein-membrane association with respect to [B]

σ – Surface density of membrane-bound protein per lipid

$K_{n,iS}$ – Dissociation constant describing association of a protein with a lipid ensemble binding site composed of *n* total lipid, *i* of which are *S*

K_l^{eff} – Effective dissociation constant describing association of protein with a lipid ensemble binding site in which there are *l* number of preferred contacts with *S*

q – The maximum number of lipid contacts in the lipid ensemble binding site for which the protein prefers *S* over *C*

θ_{Site} – Bound fraction of binding sites on a protein that associates with soluble ligands

h_{site} – Hill number describing the cooperativity of a protein that associates with soluble ligands

h_{memb} – Membrane- Hill number describing the in-plane cooperativity of a protein for the preferred lipid *S*

K_h - Apparent dissociation constant associated with the Hill approximation

DIVALENT CATION BINDING PARAMETERS

$K_{D,L,Ca^{2+}}$ – Dissociation constant of protein-cation-membrane association with respect to [L] and $[Ca^{2+}]$

$K_{l,m}^{eff}$ – Effective dissociation constant describing association of a protein-cation complex containing *m* number of divalent cations (m = 1 is represented with the subscript Ca^{2+}) with a lipid ensemble binding site in which there are *l* number of preferred contacts with *S*

$K_{Ca^{2+},m}$ – Dissociation constant of protein-cation association with respect to $[Ca^{2+}]$ for *m* number of divalent cations

$h_{memb,Ca^{2+},m}$ – Membrane-Hill number describing the in-plane cooperativity of a protein-cation complex containing *m* number of divalent cations for the preferred lipid *S*

$h_{Ca^{2+},S}$ – Hill number describing the cooperativity of the protein-cation-membrane complex for the divalent cation

EC50 – Concentration of divalent cation that induces half-maximal membrane association of the protein at fixed values of [L] and {S}

protein kinase C (PKC), as well as lactadherin, annexins, synaptotagmins, and transmembrane immunoglobulin and mucin (TIM) domain-containing proteins, have all demonstrated to be sensitive to the amount of membrane PS (12–31). The affinity of peripheral proteins for different membrane compositions has been characterized by a variety of experimental techniques (32–34). Typically, binding affinity is measured by varying the aqueous concentration of vesicles, proteins, or small ligand mediators such as divalent cations. Compositional dependence is often inferred from the variance of these measured affinities across different membrane compositions. However, comparisons of these disparate affinities obtained from diverse studies are difficult to evaluate. This is because there is no consensus model that relates the binding parameters obtained from different approaches. Rather, binding equations are either applied ad hoc or are derived for only specific cases in each study (13,14,17,20,21,30,31,35,36).

Consequently, it is difficult to determine the sensitivity of a given protein to a particular lipid species much less compare the sensitivities of multiple proteins. Furthermore, a thorough investigation of lipid composition dependence requires experiments with many membrane conditions, which can be prohibitively expensive uses of time and resources. A systematic approach is needed to efficiently characterize the determinants of such interactions.

To that end, we present a way to integrate the results of multiple binding experiments so as to provide a holistic description of the dependence of protein binding on lipid

composition. The model and its associated binding equations are significantly different from customary approaches. It presents a new way to analyze seemingly cooperative interactions involving multiple lipid species as made manifest in sigmoidal binding isotherms. Additionally, the model is consistent with standard analyses employed in the literature and predicts the lipid composition dependence of their respective parameters. The involvement of divalent cations that often coordinate protein and lipid interactions is also considered, and the application of this model to published data provides useful insights.

MATERIALS AND METHODS

Data were analyzed with a two-stage least squares fitting procedure and plotted using a combination of custom MATLAB code (37) and GraphPad Prism (38), as described in Kerr et al. (26) and Suwatthee et al. (39).

RESULTS

Model preliminaries and background

The affinity of peripheral proteins is usually determined as a function of the concentration of either the lipid or the protein. For monomeric peripheral proteins, single-site binding equations, the equilibrium-binding parts of the Michaelis-Menten or Langmuir Adsorption Isotherm equations, are typically used to analyze data (35,40). An apparent dissociation constant describing the affinity with respect to the lipid concentration, $K_{D,L}$, is obtained from such an analysis using the following single-site binding equation:

$$\frac{[\mathrm{P}]_{\mathrm{bound}}}{[\mathrm{P}]_{\mathrm{tot}}} = \frac{[\mathrm{L}]}{K_{D,L} + [\mathrm{L}]}, \tag{1}$$

where $[\mathrm{P}]_{\mathrm{bound}}$ is the concentration of the bound protein, $[\mathrm{P}]_{\mathrm{tot}}$ is the total concentration of protein, and [L] is the concentration of lipid unassociated with protein (all concentrations in square brackets are in moles/liter aqueous medium). Eq. 1 assumes that the unbound lipid is in great excess to the protein. Such experiments are conducted with a fixed total concentration of protein and by varying the total amount of lipid, assuming a fixed lipid composition.

Similarly, an apparent dissociation constant describing the affinity with respect to the concentration of protein is obtained from the single-site binding equation:

$$\frac{[\mathrm{P}]_{\mathrm{bound}}}{[\mathrm{P}]_{\mathrm{bound,max}}} = \frac{[\mathrm{P}]}{K_{D,P} + [\mathrm{P}]} \tag{2}$$

Here, [P] is the concentration of free protein and $[\mathrm{P}]_{\mathrm{bound,max}}$ is the maximum concentration of bound protein at saturation. While Eq. 1 describes the fraction of protein bound to the membrane, Eq. 2 describes the fractional saturation of the membrane surface. Analogous to Eq. 1, Eq. 2 is only valid when the protein is in great excess to lipid.

The dissociation constants, $K_{D,L}$ and $K_{D,P}$ can be used to compare the preference of a given protein for membranes of different compositions. However, it is not clear how these dissociation constants relate to one another, nor do they reflect the complex dependence on the membrane composition. These equations describe binding with a homogeneous ligand, but the membrane surface is a heterogeneous collection of lipids that should presumably have different free energies of association. Furthermore, these proteins do not bind to all or just any of the lipids, but to specific subsets thereof. These complexities not only impede the comparison of these dissociation constants but also obfuscate their fundamental interpretations.

In the following section, we derive a single expression that describes protein binding as a function of heterogeneous collections of lipids. This approach is applied to proteins that utilize divalent cations and anionic lipids.

Construction of the model

We assume a monolayer or single leaflet of a bilayer in which the lipids are in rapid diffusional equilibrium. We assume that the membrane-binding interface of the protein is large enough to facilitate direct contacts with multiple lipids. This contact site acts as the ligand and will henceforth be designated as the membrane-binding site, B.

A novel aspect of our model is the characterization of peripheral protein binding in terms of compound lipid contact sites created by protein binding. Naturally, the lipid configuration of these contact sites varies and depends on the composition of the bulk membrane. In turn, the bound protein exists in an ensemble of bound states distinguished by their contact site configurations. We let [PB] represent the concentration of the ensemble of protein-binding site complexes, and [P] represent the free protein. We define $[\mathrm{PB}]_{\mathrm{max}}$ as the concentration of the membrane-bound protein when the membrane is saturated. Under non-saturating conditions, we can define an effective concentration of these unbound lipid ensembles as $[\mathrm{B}] = [\mathrm{PB}]_{\mathrm{max}} - [\mathrm{PB}]$. The free protein, [P], and free membrane-binding sites, [B], are in equilibrium with the ensemble of protein-bound membrane-binding sites, [PB], described by the following dissociation constant:

$$K_{D,B} = \frac{[\mathrm{P}][\mathrm{B}]}{[\mathrm{PB}]} \tag{3}$$

For a more nuanced and technical description of lipid ensemble membrane binding sites, see Appendix A. The binding equations for the bound fraction of protein and the fraction of total membrane-binding capacity are, respectively:

$$\frac{[\mathrm{PB}]}{[\mathrm{P}]_{\mathrm{tot}}} = \frac{[\mathrm{B}]}{K_{D,B} + [\mathrm{B}]} \tag{4}$$

$$\frac{[\mathrm{PB}]}{[\mathrm{PB}]_{\max}} = \frac{[\mathrm{P}]}{K_{D,B} + [\mathrm{P}]} \tag{5}$$

Note that $K_{D,B} = K_{D,P}$ of Eq. 2 because the contact site is defined in a one-to-one stoichiometry with the protein. The relationship of $K_{D,B}$ to $K_{D,L}$ is not immediately evident, as [B] in Eq. 4 denotes the contact site while [L] in Eq. 1 denotes lipids. However, if on a saturated membrane the bound protein is present at a surface density per lipid, σ, then we can infer that each protein associates with $^1/_\sigma$ number of lipids. We therefore scale the concentration of lipid ensembles, [B] to the concentration of free lipid, [L] , with the parameter, σ. That is,

$$[\mathrm{B}] = \sigma[\mathrm{L}] \tag{6}$$

Substituting σ[L] for [B] in Eq. 4 shows that $K_{D,L}$ differs from $K_{D,B}$ by a factor of σ:

$$\frac{[\mathrm{PB}]}{[\mathrm{P}]_{\mathrm{tot}}} = \frac{[\mathrm{L}]}{K_{D,L} + [\mathrm{L}]} \tag{7}$$

$$K_{D,B} = \sigma K_{D,L} \tag{8}$$

The parameter σ represents the inverse of the average number of lipids in the contact site. The values of both σ and $K_{D,B}$ (or, equivalently, $K_{D,L}$ or $K_{D,P}$) depend on the lipid composition, temperature, pressure, and buffer conditions. Note that σ does not directly appear in either binding equation, Eqs. 5 or 7. Its contribution primarily manifests in the comparison of dissociation constants obtained from experiments that measure the bound fraction of protein as in Eq. 7 (e.g., using tryptophan fluorescence or fluorescence polarization) with those that measure fractional membrane saturation as in Eq. 5 (e.g., using surface plasmon resonance or fluorescence microscopy). See Appendix A for a deeper discussion on σ. Without any loss of generality, we focus on experiments that measure the bound fraction of protein as in Eq. 7 and derive an analytical expression for the lipid composition dependence of its corresponding dissociation constant $K_{D,L}$.

The principal difference between the treatment of binding by proteins of water-soluble ligands and those that are membrane-bound is that the latter is a composite ligand that engages the protein in an ensemble of multiple configurations. Our model is built on the assumption that these many configurations each has its distinct affinity that, through their ensemble average, provides an emergent dependence on the lipid composition. The apparent dissociation constants for the ensemble average binding site of Eqs. 5 and 7 will represent the sum of all such unique membrane configurations weighted by their respective affinities.

We first consider a membrane composed of only two lipid species, C and S, the latter of which the protein associates with higher affinity. A given "binding site" has n total lipids, i of which are S and $n - i$ are C. Its corresponding affinity for P is given by the dissociation constant, $K_{n,iS}$, where the subscripts denote the number of total lipids, n, and the number of S in the "binding site," i, as illustrated in the cartoon in Fig. 1*a*. We obtain $K_{D,L}$ by summing over all compositions of the binding site and all binding site sizes, n, up to N total lipids.

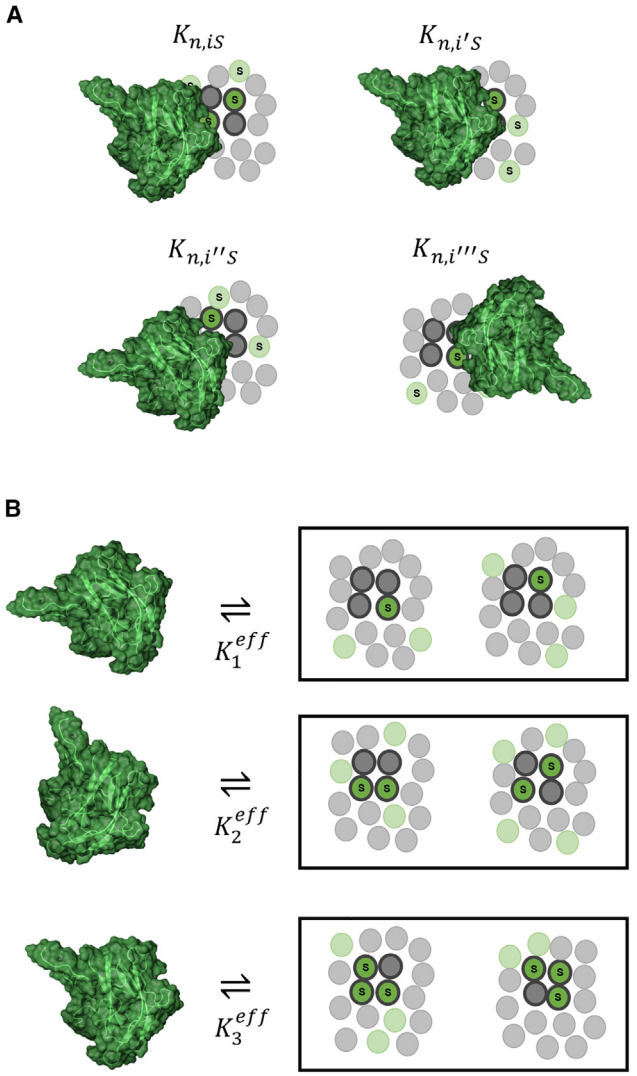

FIGURE 1 Hypothetical modes of membrane association by a protein. (*a*) Each unique configuration of lipids has a different affinity for the protein given by the dissociation constant, $K_{n,iS}$. n is the number of lipids contacted by the protein and i is the number of preferred species S is present in the whole binding site. All circles represent lipids that make direct contact with the protein while bold-rimmed circles represent preferred contacts in which the protein binds S with higher affinity than C while the rest have approximately equal affinity. (*b*) Eq. 11 reorganizes the configurations depicted in (*a*) into a set of binding modes based on the number of S that are preferentially contacted by the protein in each configuration. Top row: All protein states that interact with one S among its preferred sites are grouped in an ensemble with an effective dissociation constant, K_1^{eff}. The 2- and 3-S ensembles are treated similarly in the middle and bottom rows, respectively. The protein cartoon is derived from PDB: 2L9L. To see this figure in color, go online.

$$\frac{1}{K_{D,L}} = \sum_{n}^{N}\sum_{i}^{n}\frac{\{S\}^{i}\{C\}^{n-i}}{K_{n,iS}} \quad (9)$$

In its present form, this expression contains too many parameters for fitting experimental data. To reduce the number of parameters, we approximate it based on the following considerations: 1) For a subset of lipid contacts, configurations will have invariant dissociation constants under interchange of S and C, that is, only certain lipid contacts are sensitive to lipid identity (illustrated in Fig. 1*a* as thicker rimmed circles). 2) The contributions of individual configurations to the observed binding are indiscernible. However, subensembles of configurations with the same $\{S\}$ and $\{C\}$ dependence do have discernible influence. Based on these two considerations, we derived the following expression in Appendix A:

$$\frac{1}{K_{D,L}} = \sum_{n}^{N}\sum_{i}^{n}\frac{\{S\}^{i}\{C\}^{n-i}}{K_{n,iS}} \approx \sum_{l}^{q}\frac{\{S\}^{l}}{K_{l}^{\mathrm{eff}}} \quad (10)$$

Here, q represents the maximum number of S that the protein prefers over C in the binding site. Based on the first consideration above, we generally expect $q < N$. For example, a given protein bound to $n = 20$ lipids might only preferentially associate up to 5 S while being indifferent to whether the remaining 15 contacts are S or C. The index, l, labels the number of S among the preferred contacts, while i counts the total number of S among all contacts in the binding site. Eq. 10, therefore, reduces the number of parameters to $q + 1$ (including the state with zero preferred S). The value of q should be determined by regression. In this expression, K_{l}^{eff} represents effective dissociation constants for ensembles of bound configurations with l preferred S in the "binding site," as illustrated in the cartoon of Fig. 1*b*. If, contrary to assumption, S is not uniformly preferred over C, Eq. 10 is still valid but the values of K_{l}^{eff} can be negative. To allow for this possibility, K_{l}^{eff} should not be constrained to be positive in regression. Consequently, K_{l}^{eff} does not correspond to a free energy; see Appendix A for more information.

By substituting $K_{D,L}$ in Eq. 7, we obtain an expression for the bound fraction of protein:

$$\frac{[\mathrm{PB}]}{[\mathrm{P}]_{\mathrm{tot}}} = \frac{[\mathrm{L}]\sum_{l}^{q}\frac{\{S\}^{l}}{K_{l}^{\mathrm{eff}}}}{1+[\mathrm{L}]\sum_{l}^{q}\frac{\{S\}^{l}}{K_{l}^{\mathrm{eff}}}} \quad (11)$$

We call Eq. 11 the "single-species membrane-binding equation," reflecting its dependence on the composition of the single-species S. Even with complex lipid compositions, Eq. 11 allows us to characterize the dependence on S alone, as if S were the only ligand. If needed, the definition of C can be expanded to include multiple lipid species as long as their relative proportions are not varied alongside $\{S\}$. Varying this composition of background lipids, C, can tune other membrane properties such as the lipid packing density, curvature, and density of defects. The values of K_{l}^{eff} obtained for different background compositions can be compared to evaluate how the $\{S\}$-dependence varies with membrane properties. Alternatively, Eq. 11 can be extended to track the dependence on multiple, distinct lipid species (see discussion).

Altogether, this model provides a picture of membrane association that separates the interaction into several binding modes, indexed by l. These binding modes are defined as the set of configurations that preferentially interact with l number of S (e.g., zero S, one S, two S, and so on). While the explicit dependence on C is absent in Eq. 11, the values of K_{l}^{eff} implicitly depend on it. These values cannot be assumed to describe the $\{S\}$-dependence for membranes composed of lipids other than C.

As always, reality can be more complex than the models that represent it. The different binding modes might differentially contribute to the measurement output such that the bound fraction of protein is not directly reported. We discuss such a case in Appendix B, where we describe how to normalize the measurement output in order to reliably obtain the bound fraction of protein. Additionally, K_{l}^{eff} may not be constant with respect to the concentration of S. For example, a substantial increase in the amount of S may alter the physical properties of the membrane. While the constancy of K_{l}^{eff} is generally expected, we nonetheless warn experimenters to practice caution.

Application of the model: MFG-E8

We used the single-species membrane-binding equation (Eq. 11) to analyze a recently published analysis of the association of MFG-E8 with vesicles composed of various ratios of 1-palmitoyl-2-oleoyl-sn-glycero-3-phosphocholine (POPC) and 1-palmitoyl-2-oleoyl-sn-glycero-3-phosphatidylserine (POPS) (39). PS is required by MFG-E8, so we labeled it our lipid of interest, S. Binding was shown to increase with both total vesicle concentration, reported as total lipid concentration $[\mathrm{L}]$, and the membrane mole fraction of POPS, $\{S\}$ (Fig. 2 *a*). All data were fit with Eq. 11 using only a single set of parameters for all values of $[\mathrm{L}]$ and $\{S\}$ (Table 1). We observed single-site binding dependence with respect to total lipid concentration for all membrane compositions (Fig. 2*a*). These data were also plotted as a function of the PS mole fraction in Fig. 2*b*. A sigmoidal binding curve is observed for each total lipid concentration, consistent with the polynomial dependence on $\{S\}$ in Eq. 11. Sigmoidal dependence is a hallmark of positive cooperativity, in which the association of a ligand with a protein promotes subsequent associations.

Note, however, that the degree of sigmoidicity as seen in Fig. 2*b* changes as a function of the total lipid concentration. While Eq. 11 predicts this trend, it is not clear which feature of Eq. 11 is the cause. We therefore sought to formally characterize the nature of the cooperativity for lipid composition dependence inherent to Eq. 11.

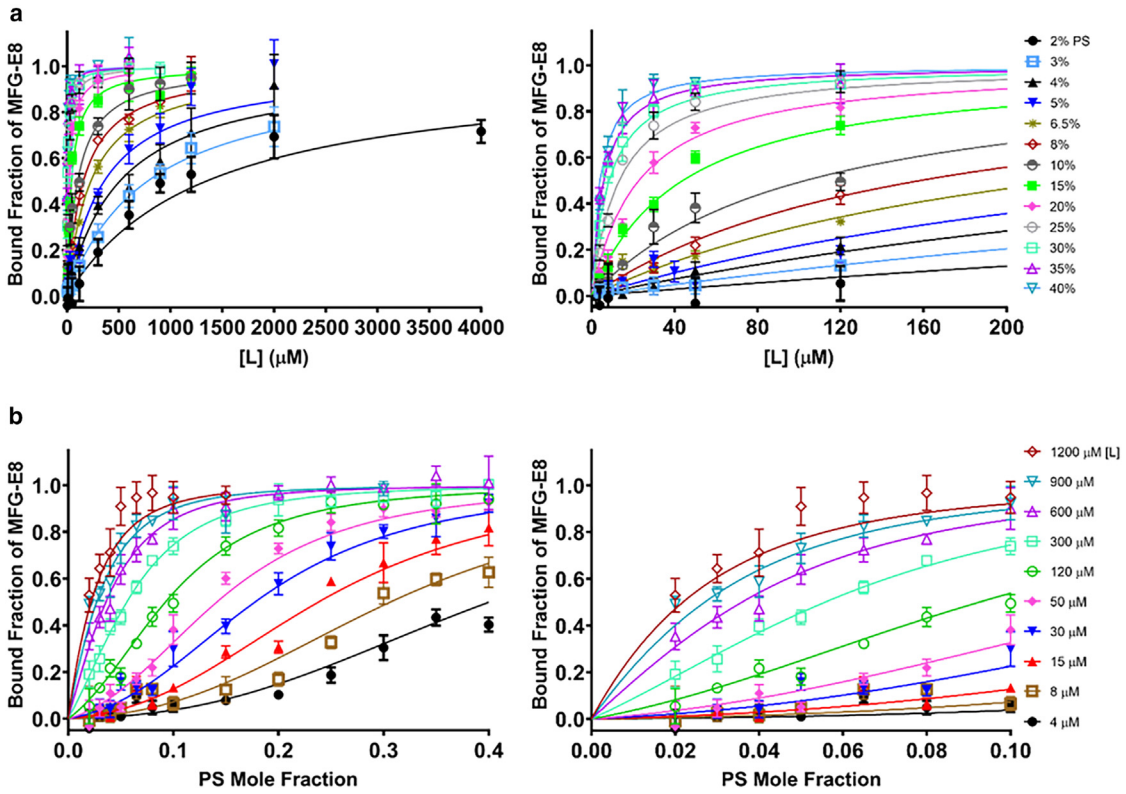

FIGURE 2 (*a*) Dependence of MFG-E8 binding to vesicles composed of varying mol% POPS and POPC as a function of the free lipid concentration, [L], which we take to be equal to the total lipid concentration given that the lipid is in great excess to the protein. The left panel depicts the binding dependence over the full measured range, while the right panel only depicts the binding at low lipid concentrations. Each curve is hyperbolic, suggesting a single-site binding dependence. (*b*) The same in panel (*a*) re-plotted as a function of POPS mol% for each lipid concentration. The left panel depicts the binding dependence over the full measured range of PS mole fraction while the right panel depicts the binding only at low PS mole fractions. All data were obtained at a total protein concentration of [P] = 80 nM. All data points represent the mean of at least three independent measurements. Error bars in all panels represent standard errors of the mean. All curves in both panels were generated using the parameter values in Table 1 obtained from the fit to the data using Eq. 11. Reproduction of data from Suwatthee et al. (39). To see this figure in color, go online.

Cooperativity from multiple binding modes

Cooperativity in ligand binding, characterized by sigmoidal binding curves, generally signifies that the association of a protein with one alters its affinity for additional ligands (41–43). This cooperativity is mediated by structural changes in the protein induced by the accommodation of ligands. The mechanism underlying cooperativity in membrane binding is fundamentally different. The ligands of a peripheral protein are highly concentrated and can facilitate multiple connections. Unlike soluble ligands, lipids are physically coupled in membranes. The protein-membrane complex is not formed from a sequence of equilibrated intermediates but instead from a single equilibration with the whole membrane interface. While it makes sense to analyze solution ligand binding in terms of spatially distinct binding sites that are sequentially liganded, this picture does not extend to peripheral membrane-binding proteins.

We present an approach to analyzing membrane-based cooperativity derived from the analysis of solution-based cooperativity. In the latter, the Adair equation describes the association of a protein with n number of ligand binding sites (44,45):

$$\theta_{site} = \frac{\sum_{i=1}^{n} i \frac{[\mathrm{L}]^i}{K_i}}{n\left(1 + \sum_{i=1}^{n} \frac{[\mathrm{L}]^i}{K_i}\right)} \tag{12}$$

In the Adair equation, [L] is the concentration of soluble ligand, i is the number of protein binding sites occupied by ligand, and θ_{site} is the fraction of *spatially distinct binding sites on the protein* occupied by ligand. Eq. 11 resembles the Adair equation (Eq. 12) in that both describe binding as an ensemble of partially liganded states with distinct affinities. In Eq. 11, these partially liganded states instead correspond to states each with a different preferred number of contacts with S. Most importantly, the Adair equation differs from Eq. 11 in tracking the fractional occupancy of ligand binding sites on the protein, θ_{site}, rather than the fraction of bound protein, $[\mathrm{PB}]/[\mathrm{P}]_{\mathrm{tot}}$.

TABLE 1 Effective dissociation constants determined for MFG-E8 binding to POPS-containing vesicles and their 95% confidence intervals

K_1^{eff}	40 μM [20, 80]
K_2^{eff}	2 μM [1, 19]
K_3^{eff}	0.4 μM [0.2, 0.8]

Data from Suwatthee et al. (39) plotted in Fig. 2 were fit by regression of Eq. 11. The number of K_l^{eff} parameters was determined to be $q = 3$ by adding more parameters until an F-test failed to reject the null hypothesis with a p value ≤ 0.05.

The cooperativity of the Adair equation is typically quantified using the Hill number, h_{site} (45–48):

$$h_{site} = \frac{\mathrm{d}}{\mathrm{d}\ln[\mathrm{L}]}\ln\left(\frac{\theta_{\mathrm{Site}}}{1-\theta_{\mathrm{Site}}}\right) \tag{13}$$

If the Hill number is greater than unity, then the affinity for subsequent ligands increases and binding is positively cooperative. Its maximum possible value is n, the number of binding sites on the protein. Conversely, a value less than unity indicates that the affinity decreases for subsequent ligand and the binding is negatively cooperative. If the value is unity, then each binding site is independent, and the binding is non-cooperative. If h_{site} is approximately independent of [L], then it can be assumed to be a constant in Eq. 13 such that solving for θ_{site} yields:

$$\theta_{site} = \frac{[\mathrm{L}]^{h_{site}}}{K_h + [\mathrm{L}]^{h_{site}}}, \tag{14}$$

where K_h is an apparent dissociation constant. Eq. 14 is called the Hill equation and, here, the constant h_{site} is called the Hill coefficient (45,46). This equation is often used due to its simplicity, featuring only two parameters, and the clear interpretation of the value of h_{site}. Since $h_{site} \leq n$, its value can be used as a lower bound estimate for the number of binding sites on a protein.

In the case of membrane binding, cooperativity is instead inferred from the fraction of protein associated with the membrane, $[\mathrm{PB}]/[\mathrm{P}]_{\mathrm{tot}}$, rather than the fractional occupancy of binding sites, θ_{site}. We call this measure of membrane-based cooperativity the Membrane-Hill number, h_{memb}:

$$\begin{aligned} h_{memb} &= \frac{\mathrm{d}}{\mathrm{d}\ln\{\mathrm{S}\}}\ln\left(\frac{[\mathrm{PB}]/[\mathrm{P}]_{\mathrm{tot}}}{1-[\mathrm{PB}]/[\mathrm{P}]_{\mathrm{tot}}}\right) \\ &= \frac{\sum_{l=0}^{q} l\frac{\{\mathrm{S}\}^l}{K_l^{\mathrm{eff}}}}{\sum_{l=0}^{q}\frac{\{\mathrm{S}\}^l}{K_l^{\mathrm{eff}}}} = \langle l\rangle_{bound} \end{aligned} \tag{15}$$

Eq. 15 is a formula for the average number of preferred associations with S, denoted as $\langle l\rangle_{bound}$, weighted by the affinity of each binding mode for the membrane. The Membrane-Hill number therefore reports the average number of preferentially associated S per protein as a function of $\{\mathrm{S}\}$. As $\{\mathrm{S}\}$ increases in the membrane, the higher-order modes are more likely to be populated. As $\{\mathrm{S}\}\to 1$, the maximum possible value it can reach is q, corresponding to all membrane-bound proteins engaging in the $l = q$ binding mode, but it may not necessarily attain this maximum at $\{\mathrm{S}\} = 1$.

(The Membrane-Hill number is mathematically equivalent to q multiplied by the Adair equation [Eq. 12] for a protein with q number of binding sites in the variable $\{\mathrm{S}\}$ [instead of [L]] and with $K_l = K_l^{\mathrm{eff}}/K_0^{\mathrm{eff}}$. This correspondence only holds for nonzero $K_0^{\mathrm{eff}-1}$, that is, for proteins that interact with C in the absence of S. Nonetheless, its interpretation as an average number of preferred contacts is analogous to a fractional occupancy of binding sites.)

Note that Eq. 15 only depends on $\{\mathrm{S}\}$ while its corresponding single-species membrane-binding equation, Eq. 11, depends on both $\{\mathrm{S}\}$ and [L]. This further shows that protein binding at the membrane surface significantly differs from the situation for soluble ligands, in which both the Adair equation (Eq. 12) and its corresponding Hill number (Eq. 13) both only depend on [L]. In that case, an increase in [L] necessitates increased saturation alongside a shift to higher-order binding. For membrane binding, however, an increase in [L] only increases the saturation with no shift in the populations of the binding modes. This extra degree of freedom reflects the dimensionality of protein-membrane binding: The three-dimensional association with the membrane governs the overall association of the protein, but the two-dimensional organization of lipids in the membrane independently determines how the protein complexes with lipids in different binding modes.

With the full apparatus of the Membrane-Hill number, we are now equipped to explain the apparent [L]-dependence of the sigmoidicity of MFG-E8 in Fig. 2*b*: By comparing the value of the Membrane-Hill number for MFG-E8 for a given value of $\{\mathrm{S}\}$ (plotted in Fig. 3*a*) to the value of the binding curves in Fig. 2*b* at the same $\{\mathrm{S}\}$, we can explain the shape of the binding curves in terms of the underlying cooperativity. For high [L], binding inflects toward saturation at $\{\mathrm{S}\} = 0.1$ (Fig. 2*b*), while the value of the Membrane-Hill number remains below 2 (Fig. 3*a*). Thus, the binding curve reflects this lower-order, approximately linear dependence on $\{\mathrm{S}\}$ in its hyperbolic shape. For low [L], the inflection toward saturation occurs by $\{\mathrm{S}\} = 0.3$, in a region in which the Membrane-Hill number slowly increases from 2 to 3. In fact, the Membrane-Hill number never quite reaches a value of 3. Here, the higher-order power dependence on $\{\mathrm{S}\}$ is reflected in the sigmoidicity of the binding curve.

The [L]-dependence of the sigmoidicity therefore emerges from the interplay of saturation and cooperativity

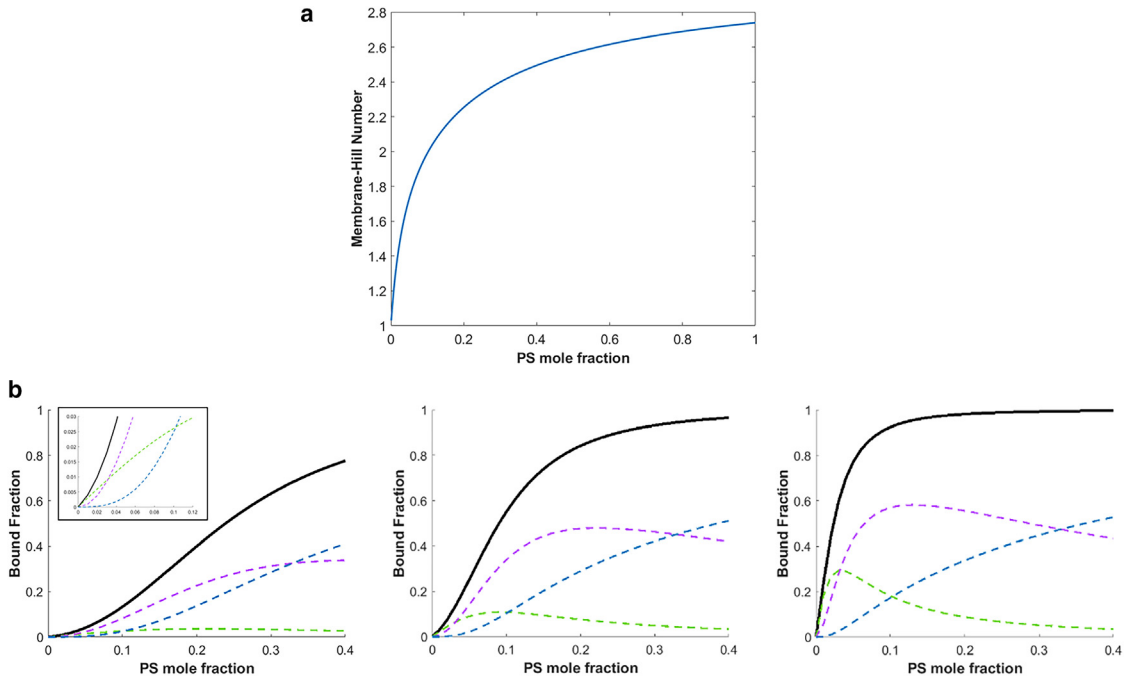

FIGURE 3 Visualizations of the PS-binding modes inferred from the fits of the data in Fig. 2. (*a*) Membrane-Hill number (Eq. 15) for MFG-E8 data as a function of PS mole fraction. (*b*) The solid black lines in the three panels represent the bound fraction in Fig. 2*b* for lipid concentrations [L] = 15, 120, and 1200 μM, respectively, while the green, purple, and blue dashed lines depict the bound fractions of the 1-PS, 2-PS, and 3-PS modes as calculated using Eq. 16. Reproduction of data from Suwatthee et al. (39). To see this figure in color, go online.

uniquely characteristic of membrane-binding. While the sigmoidicity of the curves in Fig. 2*b* seemingly depends on the free lipid concentration, this dependence is only apparent. The Membrane-Hill number (Eq. 15) is, in fact, independent of the free lipid concentration and only depends on $\{S\}$ (Fig. 3*a*). The apparent dependence of the cooperativity is best seen by visualizing each of the binding modes, PS^l, by which the protein is associated with l number of S:

$$\frac{[PS^l]}{[P]_{tot}} = \frac{[L]\frac{\{S\}^l}{K_l^{eff}}}{1 + [L]\sum_{l=0}^{q}\frac{\{S\}^l}{K_l^{eff}}} \tag{16}$$

The plots of the individual binding modes in Fig. 3*b* show two distinct features: 1) The crossover points between the binding modes occurs at the same value of $\{S\}$ for all values of $[L]$. 2) The local maxima for the $l = 1$ and $l = 2$ binding modes shift to lower $\{S\}$ and increase in bound fraction with increasing $[L]$, commensurate with overall saturation of binding at lower $\{S\}$. The binding is therefore dominated by the $l = 1$ binding mode for high $[L]$, but by the $l = 2$ mode for low $[L]$. The binding curves take on the $\{S\}$-dependence of the most populated binding mode, from which the sigmoidicity emerges.

From this analysis, we see that the Membrane-Hill number is an indicator for the distribution of binding modes. It quantifies cooperativity as the change in this distribution as a function of $\{S\}$. Its independence from $[L]$ provides an altogether different picture of binding compared with the Hill number (Eq. 13). While notions of positive and negative cooperativity are descriptive for the latter, here they cannot be consistently applied. For example, the saturation of MFG-E8 at low $\{S\}$ for high $[L]$ could be described as negatively cooperative as the higher-order modes populate only after saturation. However, the saturation at high $\{S\}$ for low $[L]$ could be described as positively cooperative since the higher-order modes populate as to increase the overall affinity for the membrane. These two cases are nonetheless described by the same set of binding parameters, obscuring the meaning of these terms. Instead, it is more meaningful to evaluate the cooperativity as the value of the Membrane-Hill number at the value of $\{S\}$ for which a given binding curve inflects toward saturation, as that most correlates with the observed sigmoidicity.

We can summarize the properties of the Membrane-Hill number as follows:

1) The Membrane-Hill number reports the average number of preferred associations with S, and, as a result, increases monotonically with $\{S\}$. Its maximum possible value is q, the total number of preferred contacts with S.
2) The Membrane-Hill number (Eq. 15) is independent of $[L]$ while its corresponding single-species membrane-binding equation, Eq. 11, depends on both $[L]$ and $\{S\}$. As a result, binding can saturate for any value of $\{S\}$. Since the Membrane-Hill number only depends on $\{S\}$, cooperativity is fully determined by interactions

within the membrane and is independent of the three-dimensional component of the interaction.

3) The appearance of positive or negative cooperativity can manifest in the same system depending on the value of [L]. A more useful descriptor is the value of the Membrane-Hill number at the inflection toward saturation. A lower number indicates a greater population of lower-order binding modes during saturation, while a higher number indicates a greater population of higher-order binding modes.
4) An observed value of unity for the Membrane-Hill number does not necessarily indicate that the protein has only one preferred contact with *S*. Binding must be measured at low enough values of [L] such that the shift of saturation to higher {S} can rule out the existence of higher-order binding modes.

Hill approximation for membrane binding

Similar to the Hill number (Eq. 13), if the Membrane-Hill number is approximately constant over the range of {S} in which binding occurs, Eq. 13 can be solved for $[PB]/[P]_{tot}$ to obtain a Hill approximation for Eq. 11:

$$\frac{[PB]}{[P]_{tot}} = \frac{[L]\{S\}^{h_{memb}}}{K_h + [L]\{S\}^{h_{memb}}} \tag{17}$$

where K_h is an apparent dissociation constant. While the Adair equation (Eq. 12) and the single-species membrane-binding equation (Eq. 11) differed significantly, the Hill approximation of the latter (Eq. 17) is mathematically equivalent to the Hill equation (Eq. 14) in the variable {S} instead of [L]. Similar to the Hill coefficient, the approximately constant Membrane-Hill number in Eq. 17 provides an estimate for the lower bound of maximum preferred associations with *S*.

The Hill approximation for membrane binding (Eq. 17) provides many benefits over Eq. 11. While Eq. 11 provides a complete description of binding by determining the effective affinities of the various binding modes, it requires a significant number of measurements for multiple values of [L] and {S} in order to robustly infer the values of K_l^{eff}. In comparison, the two parameters in Eq. 17 can be determined for a range of values of {S} and only a single value of [L].

However, the Hill approximation must be used carefully as it is valid in fewer circumstances as compared to the Hill equation for soluble ligands. As discussed in Appendix C, the constancy of the Membrane-Hill number cannot be easily assumed. In our study of MFG-E8, we found that the Hill approximation of Eq. 17 behaved poorly when simultaneously fit to all curves in Fig. 2, as seen in Fig. 4 *a*. The fit to Eq. 17 (plotted as dashed lines) undershoots the bound fraction at low {S} and high [L] but overshoots at high {S} and low [L] while the single-species membrane-binding equation, Eq. 11 (plotted as solid lines) matches these points much more closely. The inconsistent performance of the Hill approximation is intimately related to the previously observed [L]-dependence of the sigmoidicity. Indeed, as shown in Fig. 3 *a*, the Membrane-Hill number varies from 1 to 1.5 for low {S} and high [L] but skews toward 2 to 3 for high {S} and low [L], far from constant.

Since the Membrane-Hill number is approximately constant over the binding for some values of [L], the Hill approximation can instead be fit to the {S}-dependence curve for each value of [L] (Eq. 17 with unique parameter values for each value of [L]). As plotted in Fig. 4 *b*, this resulted in an improved set of fits (dashed lines) compared to the joint fit of Fig. 4 *a* that more closely agree with the fits of Eq. 11 (solid lines). These fits are well-behaved for low and high values of [L] but undershoot low {S} values for intermediate [L] (50 and 120 μM lipid in particular). The poor fits for intermediate [L] are explained by the higher variance of the Membrane-Hill number throughout the binding curves, resulting in a less valid Hill approximation.

Under low data sampling conditions, the Hill approximation (Eq. 17) can be useful. Fortunately, its invalidity is readily apparent in the quality of the fits, providing a clear diagnostic for employing Eq. 11 instead. The apparent [L]-dependence of the sigmoidicity in the MFG-E8 data also manifested as an apparent [L]-dependence in the Hill coefficient in Eq. 17 when the Hill approximation (Eq. 17) was fit to each {S}-dependence curve (39) (see Appendix C), providing an additional diagnostic for the validity of the Hill approximation. In either case, the parameters of the Hill approximation of Eq. 17 can be related to the parameters of the single-site membrane-binding equation (Eq. 11), as shown in Appendix C, and retain the interpretation of the Membrane-Hill number.

The effect of divalent cations

Eq. 11 describes the association of a protein with a single preferred lipid species, but the association of many proteins with anionic phospholipid membranes is coordinated by divalent cations. Here we denote the coordinating divalent cations as Ca^{2+}, and introduce the Ca^{2+}-dependent ensemble of membrane-bound protein complexes:

$$\frac{1}{K_{D,L,Ca^{2+}}} \approx \sum_{m=1}^{M} \sum_{l=0}^{q} \frac{[Ca^{2+}]^m \{S\}^l}{K_{l,m}^{eff}} \tag{18}$$

where $[Ca^{2+}]$ is the aqueous concentration of divalent cation, *m* is the number of divalent cations associated with the membrane-bound protein complex, and *M* is the maximal number of divalent cations that can associate with the protein. Additionally, there is an association of the soluble protein with the divalent cation:

$$\sum_{m}^{M} \frac{[P][Ca^{2+}]^m}{K_{Ca^{2+},m}} \tag{19}$$

where $K_{Ca^{2+},m}$ is the dissociation constant describing the affinity of the free protein associated with m number of divalent cations. Adding Eq. 18 to Eq. 10 and dividing by their sum with Eq. 18 results in the membrane-bound fraction of protein:

$$\frac{[\mathrm{PB}]}{[\mathrm{P}]_{\mathrm{tot}}} = \frac{[\mathrm{PL}] + [\mathrm{PCa}^{2+}\mathrm{L}]}{[\mathrm{P}] + [\mathrm{PCa}^{2+}] + [\mathrm{PL}] + [\mathrm{PCa}^{2+}\mathrm{L}]} = \frac{[\mathrm{P}][\mathrm{L}]\left(\frac{1}{K_{D,L}} + \frac{1}{K_{D,L,Ca^{2+}}}\right)}{[\mathrm{P}] + \sum_{m}^{M} \frac{[\mathrm{P}][\mathrm{Ca}^{2+}]^{m}}{K_{Ca^{2+},m}} + [\mathrm{P}][\mathrm{L}]\left(\frac{1}{K_{D,L}} + \frac{1}{K_{D,L,Ca^{2+}}}\right)} \tag{20}$$

Simplification yields:

$$\frac{[\mathrm{PB}]}{[\mathrm{P}]_{\mathrm{tot}}} \approx \frac{[\mathrm{L}]\left(\sum_{l=0}^{q} \frac{\{\mathrm{S}\}^{l}}{K_{l}^{\mathrm{eff}}} + \sum_{m=1}^{M}\sum_{l=0}^{q} \frac{[\mathrm{Ca}^{2+}]^{m}\{\mathrm{S}\}^{l}}{K_{l,m}^{\mathrm{eff}}}\right)}{1 + \sum_{m=1}^{M} \frac{[\mathrm{Ca}^{2+}]^{m}}{K_{Ca^{2+},m}} + [\mathrm{L}]\left(\sum_{l=0}^{q} \frac{\{\mathrm{S}\}^{l}}{K_{l}^{\mathrm{eff}}} + \sum_{m=1}^{M}\sum_{l=0}^{q} \frac{[\mathrm{Ca}^{2+}]^{m}\{\mathrm{S}\}^{l}}{K_{l,m}^{\mathrm{eff}}}\right)} \tag{21}$$

While the cation-independent ensemble has the Membrane-Hill number given by Eq. 15, the cation-dependent ensemble can exhibit different cooperativity depending on the number of associated cations. We separate these ensembles into sets according to the number of associated cations and define Membrane-Hill numbers, $h_{memb,Ca^{2+},m}$ for each set:

$$h_{memb,Ca^{2+},m} = \frac{\mathrm{d}}{\mathrm{d}\ln\{\mathrm{S}\}} \ln\left(\frac{\frac{[\mathrm{PCa}_{m}^{2+}\mathrm{L}]}{[\mathrm{PCa}_{m}^{2+}] + [\mathrm{PCa}_{m}^{2+}\mathrm{L}]}}{1 - \frac{[\mathrm{PCa}_{m}^{2+}\mathrm{L}]}{[\mathrm{PCa}_{m}^{2+}] + [\mathrm{PCa}_{m}^{2+}\mathrm{L}]}}\right) = \frac{\sum_{l=0}^{q} l\frac{\{\mathrm{S}\}^{l}}{K_{l,m}^{\mathrm{eff}}}}{\sum_{l=0}^{q} \frac{\{\mathrm{S}\}^{l}}{K_{l,m}^{\mathrm{eff}}}} = \langle l \rangle_{Ca^{2+},m} \tag{22}$$

As before, applying the Hill approximation to Eq. 21 yields Eq. 23:

$$\frac{[\mathrm{PB}]}{[\mathrm{P}]_{\mathrm{tot}}} \approx \frac{[\mathrm{L}]\left(\frac{\{\mathrm{S}\}^{h_{memb}}}{K_{h}} + \sum_{m=1}^{M} \frac{[\mathrm{Ca}^{2+}]^{m}\{\mathrm{S}\}^{h_{memb,Ca^{2+},m}}}{K_{h,mCa^{2+}}}\right)}{1 + \sum_{m=1}^{M} \frac{[\mathrm{Ca}^{2+}]^{m}}{K_{Ca^{2+},m}} + [\mathrm{L}]\left(\frac{\{\mathrm{S}\}^{h_{memb}}}{K_{h}} + \sum_{m=1}^{M} \frac{[\mathrm{Ca}^{2+}]^{m}\{\mathrm{S}\}^{h_{memb,Ca^{2+},m}}}{K_{h,mCa^{2+}}}\right)} \tag{23}$$

where $K_{h,mCa^{2+}}$ is the effective equilibrium constant for the divalent cation-dependent ensemble associated with m cations. If the cooperativity is independent of the number of associated cations, then a single parameter, $h_{memb,Ca^{2+}}$, can be used instead. Conventional Hill numbers describing the cooperativity for the divalent cation can also be defined for the protein-cation complex and the protein-cation-membrane complex, denoted as $h_{Ca^{2+}}$ and $h_{Ca^{2+},S}$, respectively. The resulting binding equation with Hill approximations for both the preferred lipid S and the divalent cation Ca^{2+} is given by:

$$\frac{[\mathrm{PB}]}{[\mathrm{P}]_{\mathrm{tot}}} \approx \frac{[\mathrm{L}]\left(\frac{\{\mathrm{S}\}^{h_{memb}}}{K_h} + \frac{\left[\mathrm{Ca}^{2+}\right]^{h_{Ca^{2+},S}}\{\mathrm{S}\}^{h_{memb,Ca^{2+}}}}{K_{h,Ca^{2+}}}\right)}{1 + \frac{\left[\mathrm{Ca}^{2+}\right]^{h_{Ca^{2+}}}}{K_{Ca^{2+}}} + [\mathrm{L}]\left(\frac{\{\mathrm{S}\}^{h_{memb}}}{K_h} + \frac{\left[\mathrm{Ca}^{2+}\right]^{h_{Ca^{2+},S}}\{\mathrm{S}\}^{h_{memb,Ca^{2+}}}}{K_{h,Ca^{2+}}}\right)} \tag{24}$$

When a single divalent cation is coordinated, the single-species membrane-binding equation is as follows:

$$\frac{[\mathrm{PB}]}{[\mathrm{P}]_{\mathrm{tot}}} = \frac{[\mathrm{L}]\left(\sum_{l=0}^{q}\frac{\{\mathrm{S}\}^{l}}{K_l^{\mathrm{eff}}} + \left[\mathrm{Ca}^{2+}\right]\sum_{l=0}^{q}\frac{\{\mathrm{S}\}^{l}}{K_{l,Ca^{2+}}^{\mathrm{eff}}}\right)}{1 + \frac{\left[\mathrm{Ca}^{2+}\right]}{K_{Ca^{2+}}} + [\mathrm{L}]\left(\sum_{l=0}^{q}\frac{\{\mathrm{S}\}^{l}}{K_l^{\mathrm{eff}}} + \left[\mathrm{Ca}^{2+}\right]\sum_{l=0}^{q}\frac{\{\mathrm{S}\}^{l}}{K_{l,Ca^{2+}}^{\mathrm{eff}}}\right)} \tag{25}$$

with a corresponding Hill approximation:

$$\frac{[\mathrm{PB}]}{[\mathrm{P}]_{\mathrm{tot}}} = \frac{[\mathrm{L}]\left(\frac{\{\mathrm{S}\}^{h_{memb}}}{K_h} + \left[\mathrm{Ca}^{2+}\right]\frac{\{\mathrm{S}\}^{h_{memb,Ca^{2+}}}}{K_{h,Ca^{2+}}}\right)}{1 + \frac{\left[\mathrm{Ca}^{2+}\right]}{K_{Ca^{2+}}} + [\mathrm{L}]\left(\frac{\{\mathrm{S}\}^{h_{memb}}}{K_h} + \left[\mathrm{Ca}^{2+}\right]\frac{\{\mathrm{S}\}^{h_{memb,Ca^{2+}}}}{K_{h,Ca^{2+}}}\right)} \tag{26}$$

Fully determining the parameters of Eq. 25 requires varying the lipid concentration, the mole fraction of the preferred lipid *S*, and the divalent cation concentration. Measuring these three axes of binding can be laborious but Eq. 25 can be fit to data from experiments that vary only the mole fraction of *S* and the concentration of divalent cation (26). Provided that the binding is measured at a value of the lipid concentration such that all binding modes contribute to the binding curve, it is possible to determine the parameters for all q binding modes. Similar to the case without divalent cation interactions, the Hill approximation of Eq. 26 is not necessarily robust for a wide range of lipid concentrations. However, the parameters in Eq. 26 can be fully determined at fixed lipid concentration by just varying the mole fraction of *S* and the concentration of cation. The values of these parameters might only be valid within an order of magnitude of the measured lipid concentration but can nonetheless provide an adequate model in this range. If it is not experimentally feasible to measure the binding at a lipid concentration for which all q binding modes are observable, the Hill approximation of Eq. 26 is preferred, since it will estimate the average binding mode occupancy for that lipid concentration.

The validity of the Hill approximation at fixed lipid concentration can be seen by rearranging Eq. 25 in terms of a single-site binding dependence for the divalent cation concentration:

$$\frac{[\mathrm{PB}]}{[\mathrm{P}]_{\mathrm{tot}}} = \left(\frac{[\mathrm{L}]\sum_{l=0}^{q}\frac{\{\mathrm{S}\}^{l}}{K_{l,Ca^{2+}}^{\mathrm{eff}}}}{\frac{1}{K_{Ca^{2+}}} + [\mathrm{L}]\sum_{l=0}^{q}\frac{\{\mathrm{S}\}^{l}}{K_{l,Ca^{2+}}^{\mathrm{eff}}}}\right)\frac{\left[\mathrm{Ca}^{2+}\right]}{\mathrm{EC50} + \left[\mathrm{Ca}^{2+}\right]} + \left(\frac{[\mathrm{L}]\sum_{l=0}^{q}\frac{\{\mathrm{S}\}^{l}}{K_l^{\mathrm{eff}}}}{1 + [\mathrm{L}]\sum_{l=0}^{q}\frac{\{\mathrm{S}\}^{l}}{K_l^{\mathrm{eff}}}}\right)\frac{\mathrm{EC50}}{\mathrm{EC50} + \left[\mathrm{Ca}^{2+}\right]} \tag{27}$$

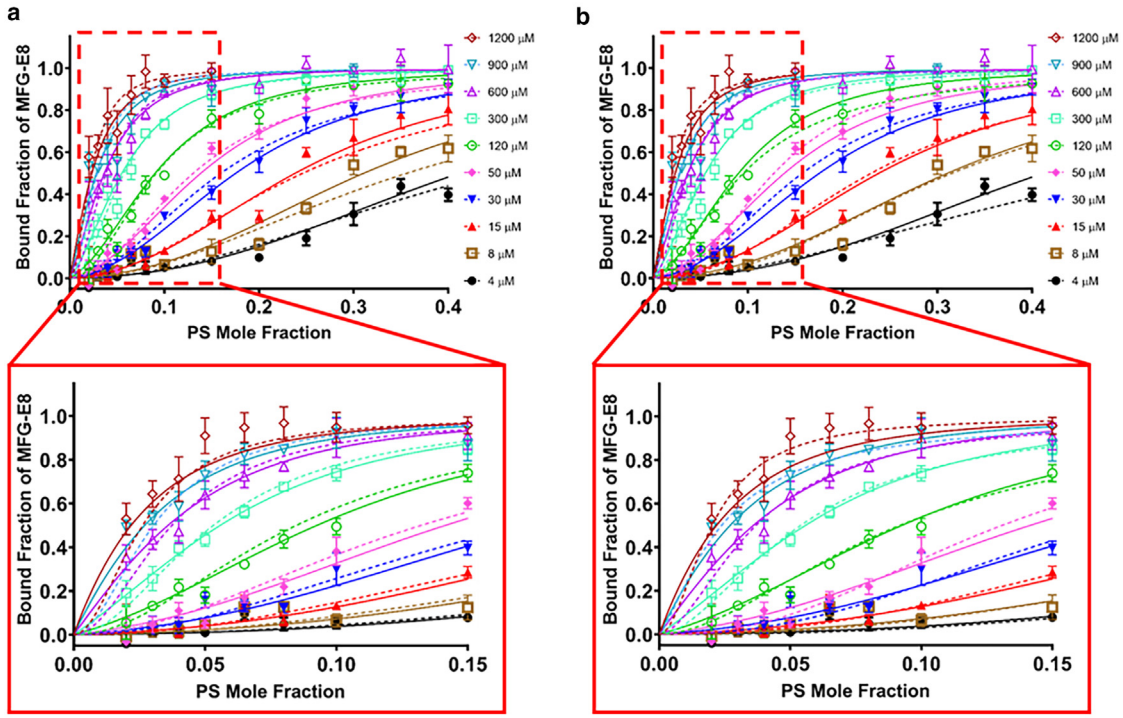

FIGURE 4 Fits of Hill approximations to the data in Fig. 2*b*. (*a*) Comparisons of the Hill equation of Eq. 17 jointly fit to all curves (dashed curves) with the single-species membrane-binding equation of Eq. 11 (solid lines) at small PS mole fractions. Error bars represent standard errors of the mean. (*b*) Comparisons of individual Hill equation fits of Eq. 17 fit to each curve (dashed curves) with those of Eq. 11 (solid lines). To see this figure in color, go online.

with the parameter EC50 denoting the concentration of the divalent cation at half-maximum binding of the protein to the membrane for fixed lipid concentration, [L], and mole fraction of the preferred lipid *S*:

$$\mathrm{EC50} = \frac{1 + [\mathrm{L}] \sum_{l=0}^{q} \frac{\{\mathrm{S}\}^l}{K_l^{\mathrm{eff}}}}{\frac{1}{K_{Ca^{2+}}} + [\mathrm{L}] \sum_{l=0}^{q} \frac{\{\mathrm{S}\}^l}{K_{l,Ca^{2+}}^{\mathrm{eff}}}} \tag{28}$$

The first parenthetical term in Eq. 27 represents the divalent cation-dependent binding ensemble in the limit of saturating divalent cation, while the second parenthetical term represents the divalent cation-independent binding ensemble in the limit of zero divalent cation. Both binding ensembles depend on the free lipid concentration and mole fraction of *S*. This equation thus describes a competitive interaction in which the divalent cation depletes the population of divalent cation-independent binding ensemble and enriches the population of the divalent cation-dependent binding ensemble with increasing divalent cation. The sigmoidicity is interpolated alongside this shift.

Fig. 5 presents data for the calcium-dependent binding of TIM3 to liposomes containing POPC and POPS as a function of either calcium concentration (Fig. 5*a*) or PS mole fraction (Fig. 5*b*). All of the curves in Fig. 5 are fit well by Eq. 25 using one set of parameters for all values of [L] and $[Ca^{2+}]$ (Table 2) and its corresponding Hill approximation, Eq. 26. Their equivalence is evident in the unchanging sigmoidicity of the TIM3 binding curves for each calcium concentration. The Membrane-Hill number varies as a function of POPS (Fig. 5*c*), but the binding curves for each calcium concentration have the same cooperativity relative to their saturation, unlike the [L]-dependence observed for MFG-E8 in Fig. 2. This can be seen in the following analysis: Since TIM3 exhibits no calcium-independent binding (shown in Fig. 5*b* for $[Ca^{2+}] = 0$ plotted as black diamonds), the calcium concentration modulates the plateaus for each {S}-dependence curve as predicted by the following reduction of Eq. 25:

$$\frac{[\mathrm{PB}]}{[\mathrm{P}]_{\mathrm{tot}}} = \left(\frac{[\mathrm{L}] \sum_{l=0}^{q} \frac{\{\mathrm{S}\}^l}{K_{l,\mathrm{Ca}^{2+}}^{\mathrm{eff}}}}{\frac{1}{K_{Ca^{2+}}} + [\mathrm{L}] \sum_{l=0}^{q} \frac{\{\mathrm{S}\}^l}{K_{l,Ca^{2+}}^{\mathrm{eff}}}} \right) \frac{[\mathrm{Ca}^{2+}]}{\mathrm{EC50} + [\mathrm{Ca}^{2+}]} \tag{29}$$

The {S}-dependence curves in Fig. 5*b* are merely instances of a single {S}-dependence curve (given by the parenthetical term in Eq. 29) scaled by the calcium isotherm (the right-hand-side term in Eq. 29). Since the parenthetical term is evaluated at a single value of [L] for each curve, they all share the same Hill approximation and, thus, a single

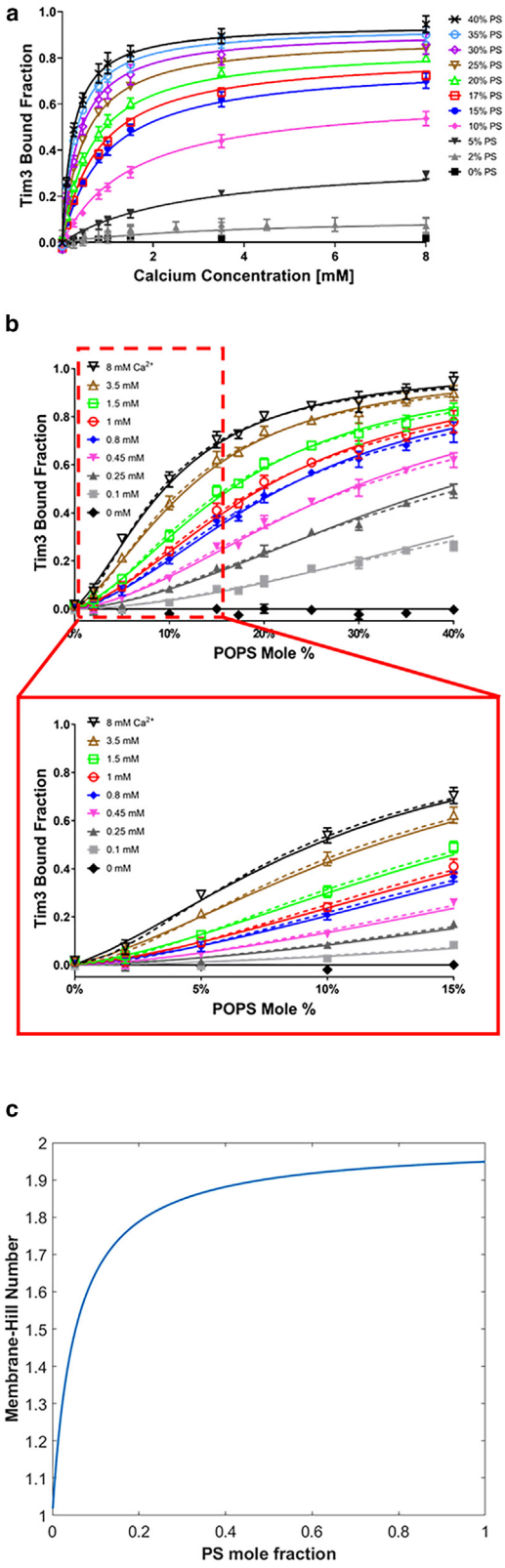

FIGURE 5 (*a*) Calcium dependence of the binding of TIM3 to vesicles composed of various compositions of POPC:POPS. (*b*) The data in (*a*) are plotted with respect to the POPS mole fraction for various calcium concentrations and expanded in the bottom panel for small POPS mole fractions. All data were obtained at a total lipid concentration of [L] = 300 μM and a total protein concentration of [P] = 170 nM. The solid lines represent a fit to Eq. 25 and dashed lines are fits of the corresponding Hill approximation (Eq. 26). Each point represents the mean of at least three independent measurements. The error bars represent standard errors of the mean. (*c*) The Membrane-Hill number of TIM3 as a function of POPS mole fraction was computed using Eq. 22 using the fit parameters of Eq. 25. Reproduction of data from Kerr et al. (26). To see this figure in color, go online.

value of $h_{memb,Ca^{2+}}$ describes the cooperativity of every curve.

(Since the calcium isotherm depends on [L] and {S} via the EC50 (Eq. 28), the calcium isotherm in Eq. 29 does not act as a simple scalar multiple of an {S}-dependence curve. However, the EC50 in the calcium isotherm is a ratio of the calcium-independent and calcium-dependent {S}-dependence curves (Eq. 28). Thus, the Hill approximation is equally valid for the {S}-dependence curves contained in the EC50 following the same argument for the parenthetical {S}-dependence curve in Eq. 29 and the Hill approximation is valid for the whole expression.)

In turn, the {S}-dependence curve in the parentheses in Eq. 29 modulates the calcium isotherm, resulting in the sub-saturating plateaus observed for the calcium dependence binding curves in Fig. 5*a*. This is caused by insufficient lipid concentration or PS mole fraction to saturate the membrane-binding of the calcium-dependent ensemble. Similarly, the dependence on S can result in sub-saturating plateaus if there is insufficient cation concentration and there is no cation-independent binding mode, as shown for TIM3 in Fig. 5*b*.

DISCUSSION

In this work, we have presented a new framework for quantifying the membrane association of peripheral membrane-binding proteins. Our model assumes the membrane-associated protein to be in an ensemble of binding states in which a few lipid contacts determine its affinity. Via this ensemble picture, the model accounts for the complex dependence on lipid composition in different physiologically relevant situations. In particular, we conceptualize lipid composition dependence in terms of distinct binding modes, each defined by the number of associations with a preferred lipid. Collectively, these binding modes can give rise to apparent cooperativity via statistical lipid occupancy of a constellation of lipid contact sites on the membrane-binding interface of the protein, even if there are no cooperative interactions between the contact sites. Both this unique source of cooperativity and the form of the resultant binding equations demand a new interpretation of membrane binding cooperativity. We showed that this cooperativity, quantified with the Membrane-Hill number, reflects the number of associations with a preferred lipid averaged over its binding modes. This contrasts with the standard view of cooperativity for

TABLE 2 Effective dissociation constants determined for TIM3 binding to Ca^{2+} and POPS-containing veiscles and their 95% confidence intervals

$K_{Ca^{2+}}$	4500 μM [3700, 5600]
$K^{eff}_{1,Ca^{2+}}$	230 μM^2 [180, 310]
$K^{eff}_{2,Ca^{2+}}$	12 μM^2 [11, 14]

Data from Kerr et al. (26) plotted in Fig. 5 were fit by regression of Eq. 25. No Ca^{2+}-independent binding was observed, so K_l^{eff} values were not fit to the data. The number of $K^{eff}_{l,Ca^{2+}}$ parameters was determined by fitting models with an increasing number of $K^{eff}_{l,Ca^{2+}}$ parameters until an F-test failed to reject the null hypothesis with a p value ≤ 0.05.

the binding of ligands to a complex in solution; namely, as a deviation in the variance of the number of occupied binding sites on a protein as compared with the same number of independent binding sites (as shown in Appendix C). We have also derived Hill approximations to reduce the number of parameters and have discussed their suitability.

Our model also can be used to derive binding equations for more complex interactions such as those involving two or more preferred lipids, cooperative divalent cation interactions, protein oligomerization, and vesicle bridging. Table 3 lists expressions for these different cases as well as their corresponding Hill approximations. The interactions listed in Table 3 can be combined to simultaneously account for multiple binding modes. For example, we accounted for both the binding of two preferred lipid species and the coordination of a single calcium ion in the TIM protein system (26). This analysis could be extended to PKCα, Synatotagmins 1 and 7, which exhibit heterotropic cooperativity for PS and phosphoinositides in the presence of calcium similar to the TIM proteins (21,27–29). However, the expressions in Table 3 should only be used when the free lipid concentration is approximately equal to the total lipid concentration (35,49). See Appendix A Eq. A16 when this approximation is not valid for the single-species membrane-binding equation (Eq. 11). Similar equations would be needed when this approximation does not hold for the cases listed in Table 3.

The subtlety of membrane binding reflected in our model requires great care in the design of experiments and their analyses. As shown in Appendix B, the output of an experiment might not directly give the bound fraction of protein. In such cases, the data must be normalized to obtain this quantity. Conversely, the dependence on divalent cations can cause the bound fraction to exhibit deviations similar to unnormalized data. However, this interaction reflects a true modulation of the bound fraction and persists even after proper normalization. The equations derived in this work clearly distinguish complications of analysis from those of the system and provide strategies to mitigate them.

Eq. 11 matches that of a previous treatment of Cytochrome P450 (14) in the single variable of the mole

TABLE 3 Dependence of the dissociation constant with respect to lipid concentration, $K_{D,L}$, for peripheral membrane-binding proteins with various interactions

Binding condition	Dissociation constant $K_{D,L}{}^{-1} \approx$	Hill approximation $K_{D,L}{}^{-1} \approx$
Single preferred lipid species, S l up to q number of preferred S	$\frac{\sum_l^q \{S\}^l}{K_l^{\text{eff}}}$	$\frac{[L]\{S\}^{h_{\text{memb}}}}{K_h}$
Two preferred lipid species, S and G l number of preferred S and j number of preferred G up to q total	$\frac{\sum_l^q \sum_j^l \{S\}^l\{G\}^j}{K_{l,j}^{\text{eff}}}$	$\frac{\{S\}^{h_{\text{memb,S}}}}{K_{h,S}} + \frac{\{S\}^{h_{\text{memb,S,G}}}\{G\}^{h_{\text{memb,G,S}}}}{K_{h,SG}} + \frac{\{G\}^{h_{\text{memb,G}}}}{K_{h,G}}$
Single preferred lipid species, S with single divalent cation, Ca^{2+} l up to q number of preferred S	$\frac{\sum_{l=0}^q \frac{\{S\}^l}{K_l^{\text{eff}}} + \sum_l^q \frac{[Ca^{2+}]\{S\}^l}{K_l^{\text{eff}}}}{1 + \frac{[Ca^{2+}]}{K_{Ca^{2+}}}}$	$\frac{\frac{\{S\}^{h_{memb}}}{K_h} + \frac{[Ca^{2+}]\{S\}^{h_{memb,C}}}{K_{h,Ca^{2+}}}}{1 + \frac{[Ca^{2+}]}{K_{Ca^{2+}}}}$
Single preferred lipid species, S with divalent cation, Ca^{2+} l up to q number of preferred S m up to M number of Ca^{2+}	$\sum_{l=0}^q \frac{\{S\}^l}{K_l^{\text{eff}}} + \frac{\sum_m^M \sum_l^q \frac{[Ca^{2+}]^m\{S\}^l}{K_{l,m}^{\text{eff}}}}{1 + \sum_m^M \frac{[Ca^{2+}]^m}{K_{Ca^{2+},m}}}$	$\frac{\frac{\{S\}^{h_{memb}}}{K_h} + \frac{[Ca^{2+}]^{h_{Ca^{2+},S}}\{S\}^{h_{memb,Ca^{2+}}}}{K_{h,Ca^{2+}}}}{1 + \frac{[Ca^{2+}]^{h_{Ca^{2+}}}}{K_{Ca^{2+}}}}$
Protein oligomerization of r, up to R, number of proteins with single preferred lipid species, S	$\sum_{r=1}^R \sum_l^q r \frac{[P]^{r-1}\{S\}^l}{K_{l,r}^{\text{eff}}}$	$\frac{[P]^{h_{prot}-1}\{S\}^{h_{memb}}}{K_{h,P}}$
Bridging of 2 membrane surfaces assuming same composition and indistinguishable membrane-binding sites with single preferred lipid species, S	$\frac{[PB]}{[P]_{\text{tot}}} = \frac{\frac{[L]}{K_{D,L,1}} + \frac{[L]^2}{K_{D,L,2}}}{1 + \frac{[L]}{K_{D,L,1}} + \frac{[L]^2}{K_{D,L,2}}}$ $\frac{1}{K_{D,L,1}} \approx \sum_l^{q_1} \frac{\{S\}^l}{K_{l,1}^{\text{eff}}}$ $\frac{1}{K_{D,L,2}} \approx \sum_l^{q_2} \frac{\{S\}^l}{K_{l,2}^{\text{eff}}}$	$\frac{1}{K_{D,L,1}} \approx \frac{[L]\{S\}^{h_{\text{memb,1}}}}{K_{h,1}}$ $\frac{1}{K_{D,L,2}} \approx \frac{[L]\{S\}^{h_{\text{memb,2}}}}{K_{h,2}}$

These expressions can be substituted into Eq. 7 to yield the dependence of the bound fraction of protein ($[PB]/[P]_{\text{tot}}$). Alternatively, these expressions can be substituted into Eq. 8 and then Eq. 5 to obtain the dependence of the bound fraction of binding sites ($[PB]/[B]_{\text{tot}}$).

fraction of the preferred lipid species. However, our approach includes the binding dependence on free lipid. The relationship between Eq. 11 and its associated Hill approximation, Eq. 17, explored in Appendix C, is similar to an approach utilized for the binding of PKC with PS (50). Additionally, PKC exhibited an apparent [L]-dependence of the sigmoidicity of PS dependence curves similar to MFG-E8 in Fig. 2*b*. Our Eq. 22 and its variants match those derived in studies of PKC, annexin, and synaptotagmins (13,17,21,30,31) in the variables of calcium concentration and lipid concentration, but our Eq. 11 also incorporates dependence on composition. The data and parameters obtained in the earlier studies are amenable to analysis using our framework and could be used in further studies of the lipid composition dependence of those proteins.

This work is broadly relevant to a variety of systems and should provide a powerful approach to the design and analysis of experiments involving peripheral membrane-binding proteins. Although we have primarily discussed proteins that associate with PS, our model can be applied to the lipid composition dependence of peripheral proteins that interact with phosphoinositides, phosphatidylcholine, phosphatic acid, phosphatidylethanolamine, sphingolipids, and other membrane constituents (4,51–56). While our work focuses on the effect of charged lipid headgroups, the framework presented here is general and can be extended to potentially characterize protein affinity for acyl chains, packing density, curvature, and other global membrane properties. This is because the model treats the binding of a protein to any collection of lipids that can be differentiated by their contribution to the affinity. The global membrane properties are not explicitly modeled in this framework, but an appropriate theory could relate the equilibrium constants defined in this model to an elastic model of the membrane such as that of Helfrich or a Gouy-Chapman model of the charged surface of the membrane (57–59). This work bridges theoretical, experimentally inaccessible equilibrium constants with those that are measured.

SUPPORTING MATERIAL

Supporting material can be found online at https://doi.org/10.1016/j.bpj.2024.02.031.

AUTHOR CONTRIBUTIONS

D.K. developed the model and derived the equations. T.S., S.M., and K.Y.C.L. provided input and feedback on the model. D.K., T.S., and S.M. designed and performed research. D.K. and T.S. analyzed data. D.K. and K.Y.C.L. wrote and edited the paper.

ACKNOWLEDGMENTS

We are grateful to Theodore L. Steck for his input, feedback, and the spark that led us on this journey. We thank Benoît Roux, Michael J. Rust, and Aaron R. Dinner for their input. This work was supported by the National Science Foundation through MCB-1950525 (to K.Y.C.L.) K.Y.C.L. acknowledges support from The University of Chicago Materials Research Science and Engineering Center (NSF/DMR-2011854) and The University of Chicago Biophysics Core Facility. T.S. is grateful for the support of The University of Chicago Chemistry and Biological Chemistry Undergraduate Summer Research Grant (2017-2018) and the Jeff Metcalf Fellowship (2019). S.M. acknowledges support from the National Institutes of Health through the CBI training grant No. 5T32GM008720-20.

DECLARATION OF INTERESTS

The authors declare no competing interests.

REFERENCES

1. Gibbons, E., K. R. Pickett, …, J. D. Bell. 2013. Molecular details of membrane fluidity changes during apoptosis and relationship to phospholipase A(2) activity. *Biochim. Biophys. Acta.* 1828:887–895.
2. Bevers, E. M., and P. L. Williamson. 2016. Getting to the outer leaflet: physiology of phosphatidylserine exposure at the plasma membrane. *Physiol. Rev.* 96:605–645.
3. Harayama, T., and H. Riezman. 2018. Understanding the diversity of membrane lipid composition. *Nat. Rev. Mol. Cell Biol.* 19:281–296.
4. Stace, C. L., and N. T. Ktistakis. 2006. Phosphatidic acid- and phosphatidylserine-binding proteins. *Biochim. Biophys. Acta.* 1761:913–926.
5. Dopico, A. M., and G. J. Tigyi. 2007. A glance at the structural and functional diversity of membrane lipids. *Methods Mol. Biol.* 400:1–13.
6. Dickey, A., and R. Faller. 2008. Examining the contributions of lipid shape and headgroup charge on bilayer behavior. *Biophys. J.* 95:2636–2646.
7. van Meer, G., D. R. Voelker, and G. W. Feigenson. 2008. Membrane lipids: where they are and how they behave. *Nat. Rev. Mol. Cell Biol.* 9:112–124.
8. van Blitterswijk, W. J., G. de Veer, …, P. Emmelot. 1982. Comparative lipid analysis of purified plasma membranes and shed extracellular membrane vesicles from normal murine thymocytes and leukemic GRSL cells. *Biochim. Biophys. Acta.* 688:495–504.
9. Sampaio, J. L., M. J. Gerl, …, A. Shevchenko. 2011. Membrane lipidome of an epithelial cell line. *Proc. Natl. Acad. Sci. USA.* 108:1903–1907.
10. Bigay, J., and B. Antonny. 2012. Curvature, lipid packing, and electrostatics of membrane organelles: defining cellular territories in determining specificity. *Dev. Cell.* 23:886–895.
11. Lorent, J. H., L. Ganesan, …, I. Levental. 2019. The molecular and structural asymmetry of the plasma membrane. Preprint at bioRxiv. https://doi.org/10.1101/698837.
12. Tait, J. F., and D. Gibson. 1992. Phospholipid binding of annexin V: Effects of calcium and membrane phosphatidylserine content. *Arch. Biochem. Biophys.* 298:187–191.
13. Tait, J. F., D. F. Gibson, and C. Smith. 2004. Measurement of the affinity and cooperativity of annexin V-membrane binding under conditions of low membrane occupancy. *Anal. Biochem.* 329:112–119.
14. Denisov, I. G., and S. G. Sligar. 2012. A novel type of allosteric regulation: functional cooperativity in monomeric proteins. *Arch. Biochem. Biophys.* 519:91–102.
15. Mosior, M., and R. M. Epand. 1993. Mechanism of activation of protein kinase C: roles of diolein and phosphatidylserine. *Biochemistry.* 32:66–75.
16. Bazzi, M. D., and G. L. Nelsestuen. 1990. Protein kinase C interaction with calcium: a phospholipid-dependent process. *Biochemistry.* 29:7624–7630.

17. Bazzi, M. D., and G. L. Nelsestuen. 1991. Highly sequential binding of protein kinase C and related proteins to membranes. *Biochemistry.* 30:7970–7977.
18. Wen, Y., R. A. Dick, …, V. M. Vogt. 2016. Effects of membrane charge and order on membrane binding of the retroviral structural protein gag. *J. Virol.* 90:9518–9532.
19. Shi, J., C. W. Heegaard, …, G. E. Gilbert. 2004. Lactadherin binds selectively to membranes containing phosphatidyl-L-serine and increased curvature. *Biochim. Biophys. Acta.* 1667:82–90.
20. Del Vecchio, K., and R. V. Stahelin. 2018. Investigation of the phosphatidylserine binding properties of the lipid biosensor, Lactadherin C2 (LactC2), in different membrane environments. *J. Bioenerg. Biomembr.* 50:1–10.
21. Tran, H. T., L. H. Anderson, and J. D. Knight. 2019. Membrane-Binding Cooperativity and Coinsertion by C2AB Tandem Domains of Synaptotagmins 1 and 7. *Biophys. J.* 116:1025–1036.
22. Corbalan-Garcia, S., and J. C. Gómez-Fernández. 2014. Signaling through C2 domains: more than one lipid target. *Biochim. Biophys. Acta.* 1838:1536–1547.
23. DeKruyff, R. H., X. Bu, …, J. M. Casasnovas. 2010. T cell/transmembrane, Ig, and mucin-3 allelic variants differentially recognize phosphatidylserine and mediate phagocytosis of apoptotic cells. *J. Immunol.* 184:1918–1930.
24. Tietjen, G. T., Z. Gong, …, E. J. Adams. 2014. Molecular mechanism for differential recognition of membrane phosphatidylserine by the immune regulatory receptor Tim4. *Proc. Natl. Acad. Sci. USA.* 111:E1463–E1472.
25. Kerr, D., G. T. Tietjen, …, K. Y. C. Lee. 2018. Sensitivity of peripheral membrane proteins to the membrane context: A case study of phosphatidylserine and the TIM proteins. *Biochim. Biophys. Acta Biomembr.* 1860:2126–2133.
26. Kerr, D., Z. Gong, …, K. Y. C. Lee. 2021. How Tim proteins differentially exploit membrane features to attain robust target sensitivity. *Biophys. J.* 120:4891–4902.
27. Landgraf, K. E., N. J. Malmberg, and J. J. Falke. 2008. Effect of PIP2 binding on the membrane docking geometry of PKC alpha C2 domain: an EPR site-directed spin-labeling and relaxation study. *Biochemistry.* 47:8301–8316.
28. Lai, C.-L., K. E. Landgraf, …, J. J. Falke. 2010. Membrane docking geometry and target lipid stoichiometry of membrane-bound PKCα C2 domain: a combined molecular dynamics and experimental study. *J. Mol. Biol.* 402:301–310.
29. Corbin, J. A., J. H. Evans, …, J. J. Falke. 2007. Mechanism of specific membrane targeting by C2 domains: localized pools of target lipids enhance Ca2+ affinity. *Biochemistry.* 46:4322–4336.
30. Almeida, P. F. F., H. Sohma, …, A. Hinderliter. 2005. Allosterism in membrane binding: a common motif of the annexins? *Biochemistry.* 44:10905–10913.
31. Kertz, J. A., P. F. F. Almeida, …, A. Hinderliter. 2007. The cooperative response of synaptotagmin I C2A. A hypothesis for a Ca2+-driven molecular hammer. *Biophys. J.* 92:1409–1418.
32. Lemmon, M. A. 2008. Membrane recognition by phospholipid-binding domains. *Nat. Rev. Mol. Cell Biol.* 9:99–111.
33. Scott, J. L., C. A. Musselman, …, R. V. Stahelin. 2012. Emerging methodologies to investigate lipid-protein interactions. *Integr. Biol.* 4:247–258.
34. Cho, H., M. Wu, …, C. Chan. 2012. Latest developments in experimental and computational approaches to characterize protein-lipid interactions. *Proteomics.* 12:3273–3285.
35. Cho, W., L. Bittova, and R. V. Stahelin. 2001. Membrane binding assays for peripheral proteins. *Anal. Biochem.* 296:153–161.
36. Frank, D. J., I. G. Denisov, and S. G. Sligar. 2009. Mixing apples and oranges: Analysis of heterotropic cooperativity in cytochrome P450 3A4. *Arch. Biochem. Biophys.* 488:146–152.
37. The MathWorks Inc. 2022. MATLAB. The MathWorks. Inc.
38. GraphPad Software 2023. GraphPad Prism. GraphPad Software.
39. Suwatthee, T., D. Kerr, …, K. Y. C. Lee. 2023. MFG-E8: a model of multiple binding modes associated with ps-binding proteins. *Eur. Phys. J. E.* 46:114.
40. White, S. H., W. C. Wimley, …, K. Hristova. 1998. Energetics of biological macromolecules part B. . Methods in Enzymology, 295. Elsevier, pp. 62–87.
41. Stefan, M. I., and N. Le Novère. 2013. Cooperative binding. *PLoS Comput. Biol.* 9, e1003106.
42. Agliari, E., A. Barra, …, S. Perrone. 2018. Complex reaction kinetics in chemistry: A unified picture suggested by mechanics in physics. *Complexity.* 2018:1–16.
43. Cattoni, D. I., O. Chara, …, F. L. González Flecha. 2015. Cooperativity in Binding Processes: New Insights from Phenomenological Modeling. *PLoS One.* 10, e0146043.
44. Adair, G. S., A. Bock, and H. Field. 1925. Others, The hemoglobin system VI. The oxygen dissociation curve of hemoglobin. *J. Biol. Chem.* 63:529–545.
45. Wyman, J. 1964. LINKED FUNCTIONS AND RECIPROCAL EFFECTS IN HEMOGLOBIN: A SECOND LOOK. *Adv. Protein Chem.* 19:223–286.
46. Holt, J. M., and G. K. Ackers. 2009. Biothermodynamics, Part A. . Methods Enzymol., 455. Elsevier, pp. 193–212.
47. Dahlquist, F. W. 1978. The meaning of Scatchard and Hill plots. *Methods Enzymol.* 48:270–299.
48. Wyman, J. 1967. Allosteric Linkage. *J. Am. Chem. Soc.* 89:2202–2218.
49. Devaux, P. F., and M. Seigneuret. 1985. Specificity of lipid-protein interactions as determined by spectroscopic techniques. *Biochim. Biophys. Acta.* 822:63–125.
50. Mosior, M., and A. C. Newton. 1998. Mechanism of the apparent cooperativity in the interaction of protein kinase C with phosphatidylserine. *Biochemistry.* 37:17271–17279.
51. Falkenburger, B. H., J. B. Jensen, …, B. Hille. 2010. Phosphoinositides: lipid regulators of membrane proteins. *J. Physiol.* 588:3179–3185.
52. Stahelin, R. V., J. L. Scott, and C. T. Frick. 2014. Cellular and molecular interactions of phosphoinositides and peripheral proteins. *Chem. Phys. Lipids.* 182:3–18.
53. Tanguy, E., N. Kassas, and N. Vitale. 2018. Protein−phospholipid interaction motifs: A focus on phosphatidic acid. *Biomolecules.* 8, 20. https://doi.org/10.3390/biom8020020.
54. Putta, P., J. Rankenberg, …, E. E. Kooijman. 2016. Phosphatidic acid binding proteins display differential binding as a function of membrane curvature stress and chemical properties. *Biochim. Biophys. Acta.* 1858:2709–2716.
55. Roberts, M. F., A. Gershenson, and N. Reuter. 2022. Phosphatidylcholine Cation-Tyrosine π Complexes: Motifs for Membrane Binding by a Bacterial Phospholipase C. *Molecules.* 27, 6184. https://doi.org/10.3390/molecules27196184.
56. Snook, C. F., J. A. Jones, and Y. A. Hannun. 2006. Sphingolipid-binding proteins. *Biochim. Biophys. Acta.* 1761:927–946.
57. Deserno, M. 2015. Fluid lipid membranes: from differential geometry to curvature stresses. *Chem. Phys. Lipids.* 185:11–45.
58. May, S., D. Harries, and A. Ben-Shaul. 2000. Lipid demixing and protein-protein interactions in the adsorption of charged proteins on mixed membranes. *Biophys. J.* 79:1747–1760.
59. Heimburg, T., B. Angerstein, and D. Marsh. 1999. Binding of peripheral proteins to mixed lipid membranes: effect of lipid demixing upon binding. *Biophys. J.* 76:2575–2586.